Interpretation of the anomalous field-cooled-magnetization behavior of high-temperature granular superconductors at low magnetic field

F. H. Chen
Department of Electronics Engineering and Institute of Electronics, National Chiao-Tung University, Hsinchu, Taiwan, Republic of China

M. F. Tai
Telecommunication Laboratories, Ministry of Transportation and Communication, P.O. Box 71, Chung-Li, Taiwan, Republic of China

W. C. Horng and T. Y. Tseng*
Department of Electronics Engineering and Institute of Electronics, National Chiao-Tung University, Hsinchu, Taiwan, Republic of China

(Received 21 December 1992; revised manuscript received 29 March 1993)

The field-cooled magnetization of high-T_c superconducting ceramics measured in low magnetic fields has exhibited an unusual phenomenon, i.e., the diamagnetic signal initially increases with a decrease in temperature but reaches a maximum at temperature T_d and subsequently decreases with a decrease in temperature. In some samples the signal could even transform inversely into a paramagnetic regime once the sample was cooled below a temperature T_p, provided the applied field was sufficiently small. This phenomenon has been observed in various high-T_c cuprates and been explained with different viewpoints. An alternative theoretical model was proposed in this work to account for these phenomena. The anomalous magnetization behavior in the present model was demonstrated to be a superposition of the diamagnetic signal, which occurs as a result of the intragranular shielding currents, and the paramagnetic signal, due to the induction of the intergranular component induced by these currents. The intergranular effect was demonstrated by this model to exist in granular superconductors. This intergranular effect would therefore be considered in evaluating the volume fraction of superconductivity for the samples from the Meissner signal, in particular, at a low magnetic field.

I. INTRODUCTION

The field dependence of the Meissner fraction[1-3] provides imperative information for constructing the H-T diagrams of the high-T_c superconductors (HTSC). For the typical characteristics of HTSC, field-cooled (FC) susceptibility (Meissner signal) is always less than zero-field-cooled (ZFC) susceptibility (shielding signal). The small Meissner fraction has been previously interpreted by the superconducting glass model[4] and flux-pinning model,[1] respectively. Nevertheless, most of the electromagnetic properties of granular HTSC are generally accepted to result from respective contributions either from the intra- or the intergranular parts or the balance exhibition of their interplays.[5] Typical FC magnetizations of HTSC at various magnetic fields can also be modeled upon consideration of the intra- and intergranular effects.[2,6]

However, an abnormal phenomenon of FC magnetization was observed by several groups[7-10] in La-, Y-, Bi-, and Tl- based superconducting systems, not realized with the typical characteristics of HTSC. This abnormal phenomenon is especially obvious in a low-field regime. Additionally, this abnormal phenomenon (shown in Fig. 1) is also exhibited by some of our measured results in the La- and Bi-based superconducting systems. This "general" anomaly considers that the sample has initially exhibited diamagnetism once cooling it below the superconducting transition temperature (T_c). The diamagnetic signal has, however, subsequently decreased with further cooling of the sample below a temperature T_d, at which the diamagnetic signal reaches maximum. The diamagnetic signal in some samples has even become invertly transformed into a paramagnetic regime when the sample was cooled below temperature T_p as long as the applied field was low enough. Various interpretations have been proposed to explain this phenomenon, including the existence of paramagnetic impurities,[7] the combination of the flux trapping capabilities of the tested material, and the inhomogeneity of the magnet in the machine,[8] the result of reversed polarity moments caused by either the clockwise or counterclockwise Josephson currents based on the superconducting glass model,[9] and the predomination of the paramagnetic part which arises as a result of the Josephson vortices over the diamagnetic part due to the shielding contribution.[10] However, among them quite limited explanations have come from these interpretations which can directly or theoretically answer the following questions. Why are the positive moments strong at a low field but weaker and weaker by increasing an applied field? Why does the T_d of positive magnetic moments monotonically decrease with an increasing applied field? Why have the positive moments in single crystals

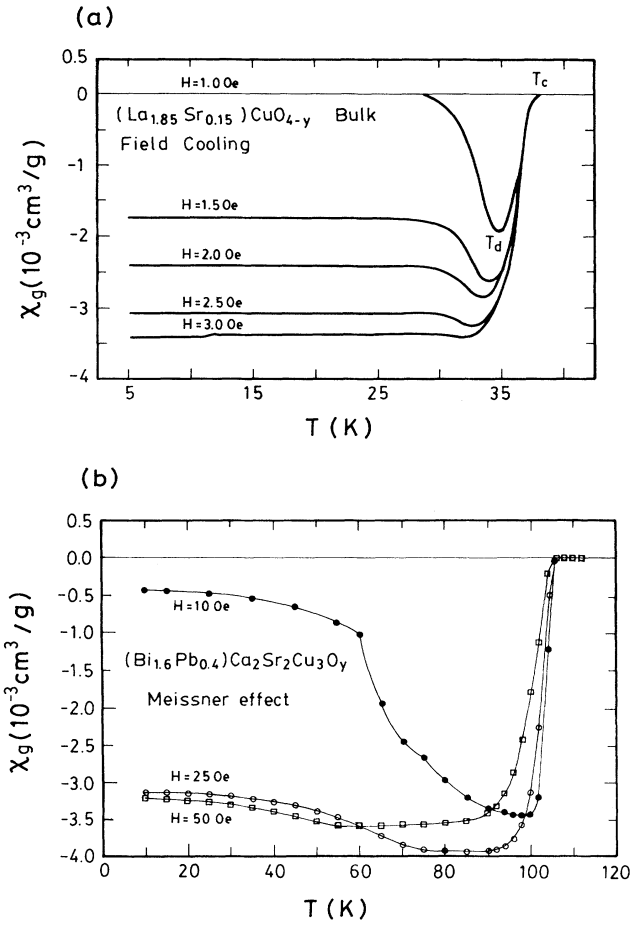

FIG. 1. Field-cooled susceptibilities of (a) La-Ba-Cu-O and (b) Bi-Sr-Ca-Cu-O, respectively.

not yet been observed in the low field even though the single crystals are known to possess lots of flux trapping centers? Why do the high-density and large-grain-size samples, e.g., Y 1:2:3 compounds[2] seldom appear at the positive moments? Why have the powders crushed from the bulk, while a large particle size could still appear at the positive moment but those with a small particle size did not?[11]

A theoretical model is proposed in this work to account for the presence of "dip" susceptibility in FC processes at low magnetic fields and disappearance at a relatively high-field regime. Above problems may be plausibly answered on the basis of our proposed model.

Quite limited research has been concentrated on investigating what would happen when the superconductors containing remarkable intergranular components are measured in magnetic fields? This is in light of the fact that these superconductors are not anticipated to have a high critical current density for the purpose of application. However, the fabrication of HTSC commonly employs the conventional ceramics processings, in which intergranular components include those pores which are parasitically present in the sample. In particular, the $YBa_2Cu_4O_8$ (1:2:4) compounds have recently been demonstrated to be capable of being prepared at normal oxygen atmosphere[12–14] instead of utilizing high oxygen pressure techniques.[15,16] The small grain size and high porosity have, however, become an unresolved problem for bulk applications of this system as a result of the requirement of low-temperature (below 820 °C) sintering at normal atmosphere, which is limited by the phase stability.[15] Nevertheless, such a "poor" sample possibly provides more manifest information concerning the effect of intergranular components on the magnetic properties of HTSC.

II. EXPERIMENTAL RESULTS

The 1:2:4 bulks were employed in this study as being the investigated system, which were straightforwardly prepared by the oxalate gel method and obtained at flowing oxygen atmosphere with the addition of sodium nitrate. After sintering, no residual sodium was detected by inductively coupled plasma and/or atomic emission spectroscopy. Sodium would therefore apparently function in a role of diffusion enhancer. The experimental procedure has been provided a detailed description elsewhere.[14]

The sample used for magnetization measurement has an orthogonal morphology with a dimension of $2a \times 2b \times c = 1 \times 2 \times 10$ mm.[3] The magnetic fields were applied in parallel with the length direction so as to minimize the effect of the demagnetic field. The scanning electron microscopy (SEM) micrograph for the sintered Na-doped 1:2:4 sample is shown in Fig. 2. The sample is porous with a density of 3.06 g/cm^3 and its average grain size is approximately 1 μm. No improvement on the microstructure arises by prolonging the sintering periods.

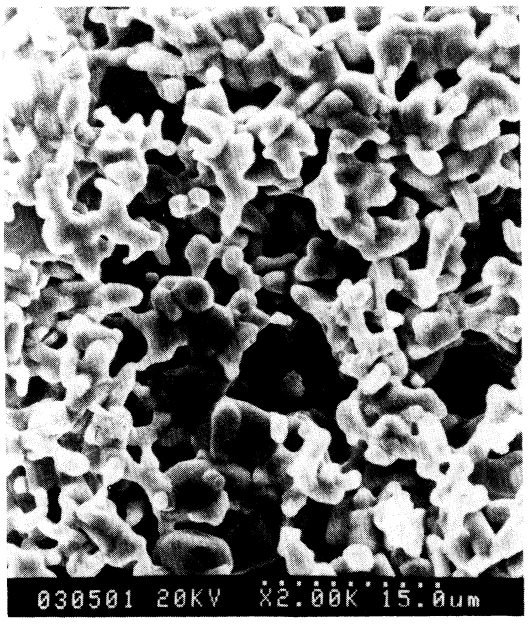

FIG. 2. The SEM micrograph for 1:2:4 compounds prepared by the sol-gel method and sintering at ambient atmosphere.

The imaginary part, $\chi''(T)$, of the ac susceptibility of a sample measured at ac magnetic field $H=H_{\rm rms}\sin\omega t$ for various $H_{\rm rms}$ values is illustrated in Fig. 3. The measurement was performed in a Lake Shore ac magnetometer. The $\chi'(T)$ curves exhibit abrupt onsets of diamagnetism at around 81 K for all fields. The diamagnetism onset temperature is in excellent agreement with the value determined by measuring the temperature vs resistance curves. No corresponding second peak is indicated in the $\chi''(T)$ curve. This is despite the fact that the $\chi'(T)$ curves measured at $h=7$ and 10 G exhibit a two-stage superconducting transition, which were also observed in Y 1:2:3 compounds[6,17] and were accounted for as a result of the effects of the intra- and intergranular components, respectively. Several possible reasons may account for the appearance of only one peak. First, the high-temperature state of $\chi'(T)$ corresponds to supercurrents inside grains. The supercurrents only flow in the surface layers without further penetration, since the lower critical field H_{c1g} of grains is higher than 7 and 10 G except for at those temperatures quite close to T_c. The loss due to grains therefore remains undetectable. The second χ'' peak may be similarly highlighted with higher fields, as shown by Skumryev, Koblischka, and Kronmüler.[18] Second, the grain size of the sintered material is small and the grain-boundary number per volume is large. The loss signal due to grains' contribution would therefore become depressed by loss signal as a result of the intergranular component. Third, as the temperatures became close to T_c, the magnetic penetration depth of the grains has been suggested by Küpfer *et al.*[19] to give rise to a suppression of the volume in which the hysteretic losses occurred. Additionally, the spatial distribution of the grains with high anisotropy has been suggested by Skumryev, Koblischka, and Kronmüler[18] to possibly decrease the χ'' maximum due to grains, since the maximum χ'' for different grains occurs at various fields and the resulting peak would be rounded off.

The complex susceptibility of the sample has been previously expressed[20] as

$$\chi=f_g\chi_g+(1-f_g)\chi_m\ , \tag{1}$$

where χ_g and χ_m are the complex susceptibilities of the grains and the matrix, respectively, and f_g is the volume fraction of the grains. If the $H_{\rm rms}$ is smaller than H_{c1g}, as the temperature is not close to T_c, $\chi_g=-1$ remains constant. Then, we can obtain

$$f_g=[\chi'_m(T_m)-\chi'(T_m)]/[1+\chi'_m(T_m)]\ . \tag{2}$$

For the sample in this study, $ba^{-1}=2$, $-\chi'_m=0.29$ is chosen here from Table II in Ref. 20. f_g estimated by $\chi'(T_m=69.7\ \text{K})$ at $H_{\rm rms}=10$ Oe is about 0.11. The small f_g implies that the material in this study consists of relatively small grains and a huge amount of pores, which is consistent with the SEM characterization.

The measurement of dc magnetization was performed in a superconducting quantum interference device magnetometer (Quantum Design MPMS). The magnetic field was set using the "no overshoot" mode, since it was undesirable for the specimen to be exposed with hysteretic behavior. The rather small fields and sample sizes in certain cases produced small signals. Special precautions therefore had to be taken to prevent or correct the spurious background signals. These special precautions were made in the light of the percent variation of the field observed by the sample being dependent on the scan length. 4-cm scan length has been applied for all dc magnetic measuring processes in this work. This scan length exhibits a field variation of only 0.19%. Three scans were operated at each temperature for enhancing statistics of data. No diamagnetic signal is indicated from Fig. 4 to have been observed above the onset temperatures, showing that the 1:2:3 phase is not present in the 1:2:4 compounds. This could account for why the dip magnetization, which has occurred in the sample measured in FC processes at the low regime field, would be of noteworthy interest. This abnormal behavior is demonstrated here in relation to the grain size and intergranular volume fraction, which is discussed in Sec. III.

III. PROPOSAL OF MODEL AND DISCUSSION

Flux lines penetrate the sample as a whole once a superconducting compound is cooled and subjected to a

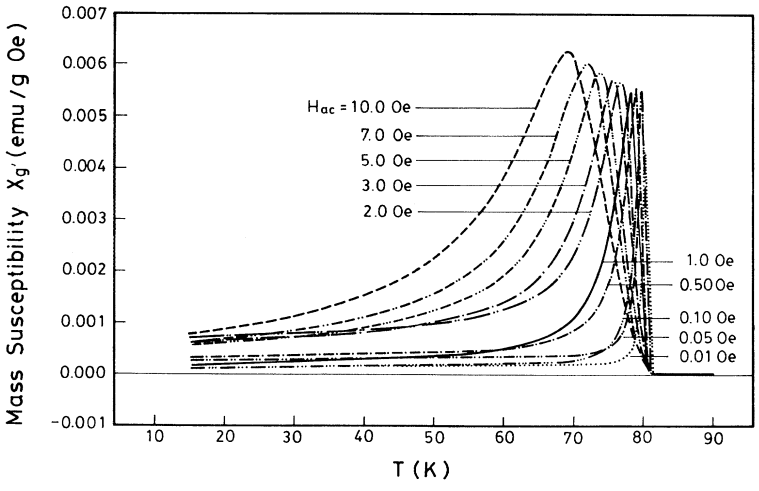

FIG. 3. The image part (χ'') of ac susceptibility of sample as in Fig. 2 measured for various $H_{\rm rms}$ values.

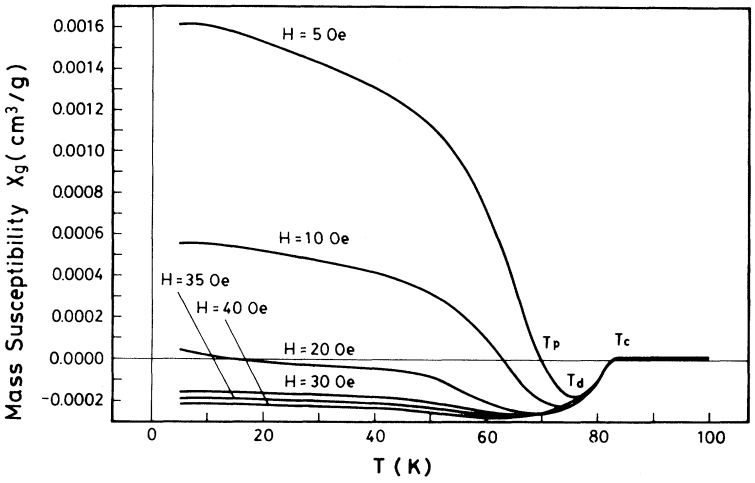

FIG. 4. The temperature dependence of the dc susceptibility of 1:2:4 compounds measured in field-cooled susceptibilities with various magnetic fields.

magnetic field and $T > T_c$. As $T < T_c$, the superconducting phase initiates nucleating inside grains as a result of the circulation of intragranular supercurrents (hereafter referred to as the GS) so as to reach the Meissner-state flux expulsion. The critical current density of grains, J_{cg}, based on the Kim's critical-state model,[6,20,21] can be approximated as

$$J_{cg}(H) \approx \alpha_g(T)/[\mu_0(H_{0g}+H)] , \tag{3}$$

where H is the applied magnetic field, $\alpha_g(T)$ the flux-pinning force density, and H_{0g} the positive constant [always less than 0.2 Oe (Ref. 6)] at a given temperature, although other functional dependencies of J_c were also previously assumed.[22–24] The subscript "g" denotes grains. For convenience, the grains are also assumed here to have the same cylindrical shape and have an identical length of L_z. Additionally, all of the center axes for grains are parallel to the applied magnetic field. Each grain with an identical radius of R_g is uniformly surrounded by the intergranular layer with a thickness of $2d_n$. Furthermore, the c axis of crystal grains is just parallel to the applied field and the GS circulate inside the grains in a-b planes with a radius of r. The GS result in the diamagnetism of the grains, but at same time also establish a paramagnetic induction in the intergranular region including pores. The effective temperature and field dependence of permeability, μ_{eff} accounting for these two parts, can therefore be expressed as

$$\mu_{\text{eff}} = f_g \left[1 - P_{\text{cyl}} \left[\frac{R_g}{\lambda_{g,ab}} \right] \right] + f_m [1 + Q_m(r)]$$
$$= 1 - f_g P_{\text{cyl}} \left[\frac{R_g}{\lambda_{g,ab}} \right] + (1 - f_g) Q_m(r) , \tag{4}$$

where $1 - P_{\text{cyl}}$ is the fractional deviation of a cylindrical grain's magnetization from a complete Meissner-state flux expulsion caused by the magnetic-flux penetration,[5] and Q_m is a factor accounting for the paramagnetic permeability of intergranular layers induced by the GS. From Ref. 25,

$$P_{\text{cyl}}(x) = 1 - 2I_1(x)/xI_0(x) , \tag{5}$$

where $I_n(x)$ is the nth-order modified Bessel's function. Thus,

$$\mu_{\text{eff}} = 2f_g \frac{I_1(R_g/\lambda_{g,ab})}{(R_g/\lambda_{g,ab}) I_0(R_g/\lambda_{g,ab})} + (1 - f_g)[1 + Q_m(r)] . \tag{6}$$

The London grain penetration depth[26] can be written as

$$\lambda_{g,ab}(t,H) \approx \lambda_{g,ab}(0)(1-t^4)^{-1/2} \times \left[1 - \frac{H}{H_{c2g}(0)} \frac{(1+t^2)}{(1-t^2)} \right]^{-1/2} , \tag{7}$$

where $t \equiv T/T_c$ is the reduced temperature. On the other hand, $Q_m(r)$ can be approximated as

$$Q_m(r) \approx \frac{\mu_0 I_{cg} r^2}{4H(R_g + d_n)^3} = \frac{\mu_0 J_{cg} \xi_{g,ab} L_z r^2}{4H(R_g + d_n)^3} , \tag{8}$$

if the condition is restricted as $(R_g + d_n)^2 \gg r^2$ (see the Appendix). We estimate r with respect to $P_{\text{cyl}}(R_g/\lambda_{g,ab})$, because it is plausible to assume that

$$\frac{\pi r^2 L_z}{\pi R_g^2 L_z} = P_{\text{cyl}} \left[\frac{R_g}{\lambda_{g,ab}} \right] , \tag{9}$$

that is,

$$r = R_g \left[P_{\text{cyl}} \left[\frac{R_g}{\lambda_{g,ab}} \right] \right]^{1/2} . \tag{10}$$

In Eq. (3), the pinning force density for the Abricosov vortices[6] is

$$\alpha_g(t) \approx H_{cg}^2(t) = H_{c1g}(0) H_{c2g}(0)(1-t^2)^2 . \tag{11}$$

With a clean-limit Ginzburg-Landau formula,[27]

$$\xi_{g,ab}(t) = 0.74 \xi_{g,ab}(0)/\sqrt{1-t} . \tag{12}$$

Substituting Eqs. (3), (7), (10), and (11) into (8), Q_m becomes a temperature and field dependence of function,

i.e.,

$$Q_m(t,H)=0.185\frac{H_{c1g}(0)H_{c2g}(0)\xi_{g,ab}(0)}{H(H+H_{0g})}\times\frac{L_zR_g^2}{(R_g+d_n)^3}(1-t)^{3/2}(1+t)^2\times P_{\rm cyl}\left[\frac{R_g}{\lambda_{g,ab}(t,H)}\right] . \quad (13)$$

The total effective permeability $\mu_{\rm eff}$ is then obtained by substituting (7) and (13) into (6). The FC magnetization can be therefore evaluated by following equation:

$$4\pi M=(\mu_{\rm eff}-1)H=\chi_{\rm eff}H , \quad (14)$$

where $\chi_{\rm eff}$ denotes the effective FC susceptibility.

Based on some magnetic measurements for Y 1:2:4 compounds,[28,29] we have chosen $\xi_{g,ab}(0)=19.5$ Å, $H_{c1g}(0)=19.7$ mT, $H_{c2g}(0)=87$ T, and $\lambda_{g,ab}(0)=1960$ Å. Actually, the effective thickness of intergranular layers, $2d_n$, can also alternatively be determined by R_g and f_g, that is,

$$2d_n=R_g\left[\left[\frac{1}{f_g}\right]^{1/2}-1\right] . \quad (15)$$

Evaluating the effective susceptibility requires only setting the values of parameters f_g, R_g, and L_z, respectively. For the sample in this study, f_g equals 0.11, R_g is approximated to be 0.5 μm, and L_z is assumed to be equal to $4Rg$. The calculated $\chi_{\rm eff}$ are plotted in Fig. 5 under various magnetic fields. Calculation results shown in Fig. 5 are observed to be similar to experimental results shown in Fig. 4. That is, as the applied field is low the diamagnetic signal initially increases and then decreases, which results in a dip susceptibility curve. The dip phenomenon gradually disappears as the applied field gradually increases. Some assumptions are notably to be made for simplifying this model, such as the shape and orientation of grain and intergranular region. These assumptions actually seldom occur at the sample prepared by common solid-state technique. This model is therefore expected to provide more qualitative than quantitative information for the conventional-sintered samples. However, this model may be used for more quantitative calculations for the grain-oriented bulks.

Relaxing the condition of small grain size and grain volume fraction, e.g., $R_g=5$ μm and $f_g=0.8$, creates a situation in which the positive moments can also appear at low-field regime, as indicated in Fig. 6. This is despite the fact that the magnetic fields are relatively low (<2.5 Oe) to observe paramagnetic signal in such a sample. This proposed model therefore plausibly verifies that the positive moments of high-granular HTSC are actually an universal phenomenon which is not abnormal at all. These positive moments are an induced paramagnetism of intergranular layers by the supercurrents inside grains. For the single crystal, f_g almost nearly equals 1; the intergranular volume fraction is then negligible and paramagnetic effect disappears, as expected by Eq. (4). The large particle size of powders crushed from the bulks are composed of a fair number of grains, which are linked by intergranular layers. The paramagnetic contribution is therefore also observable. However, for the very fine crushed powders each particle almost nearly equals one grain. The effective thickness of intergranular components can be thought of as the distance between the powders, which is always substantially larger than the powder particle size, i.e., $d_n \gg R_g$. With Eq. (8) or (13), Q_m is negligible even when the applied field is extremely low. No dip susceptibility is detected for the very fine crushed powders as the applied field becomes even small-

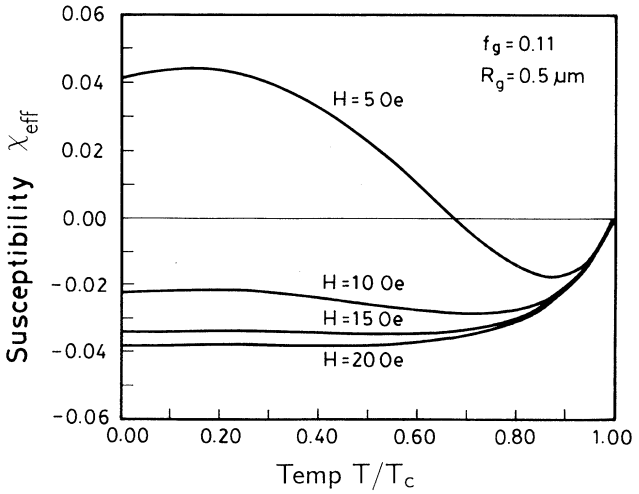

FIG. 5. The curves of the field-cooled susceptibility calculated with Eq. (14) with $R_g=0.5$ μm and $f_g=0.11$ at various magnetic fields.

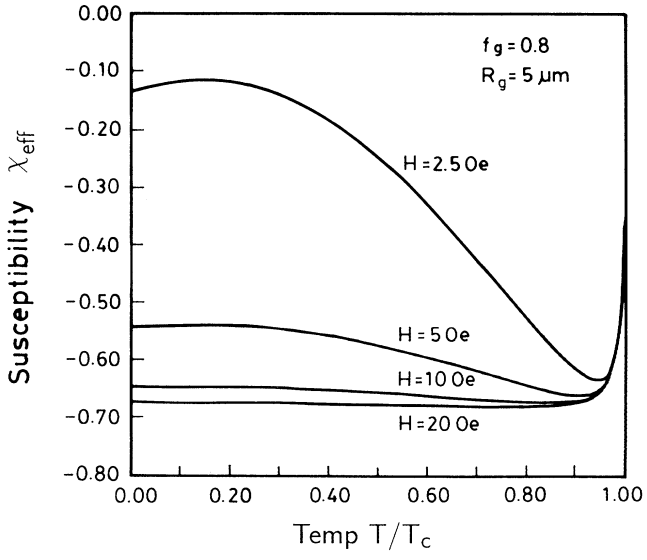

FIG. 6. The curves of the field-cooled susceptibility calculated with Eq. (14) with $R_g=5$ μm and $f_g=0.8$ at various magnetic fields.

er than 5 Oe.

The R_g and f_g dependence of χ_{eff} at a given magnetic field (5 Oe) are plotted in Figs. 7 and 8, respectively, so as to further investigate the effect of grain volume fraction and grain size on magnetization. For a small f_g, the sample with either a small or large R_g all exhibit the dip magnetization phenomenon. The dip temperature T_d increases with increasing R_g. For a large f_g, however, the dip magnetization behavior become obvious only for that sample with a large grain size. For a small R_g, the dip magnetization phenomenon has occurred at the sample with a relatively small f_g. T_d decreases with the increase of f_g. However, the large-grain-size sample shows the reduction of diamagnetic signal at a low temperature for a wide range of values for f_g, except for when f_g is close to unit. In the sample with a smaller grain volume fraction and larger grain size, the FC dip phenomenon may therefore be easier to exhibit.

To make this work more complete, some previous reports on the Y 1:2:4 granular superconductors were examined against our model. The low-field regime FC measurement (<50 Oe) for the Y 1:2:4 sample fabricated by utilizing the normal oxygen pressure technique has, to our knowledge, never been previously reported. Our considerations here must therefore be focused upon those reports using the high-pressure techniques. The grain volume fraction of the Y 1:2:4 bulks prepared by Morris *et al.*[16] having grain size ≤ 1 μm may be roughly but reasonably assumed with $0.5 \leq f_g \leq 0.8$ due to the high-pressure treatment. This sample exhibited $\chi_{\text{eff}} \approx 20\%$ at $T/T_c \approx 0.25$ and $H=6$ Oe. This result is in sufficient agreement with the small grain-size case of the present model, as indicated in Fig. 8(a). On the other hand, the samples with stoichiometric composition of $(Y_{1-x}Ca_x)Ba_2Cu_4O_8$ with $x=0$, 0.05, and 0.10, which were prepared by employing the hot isostatic pressing technique,[30] have equivalent $R_g \approx 2.5$ μm and exhibit the

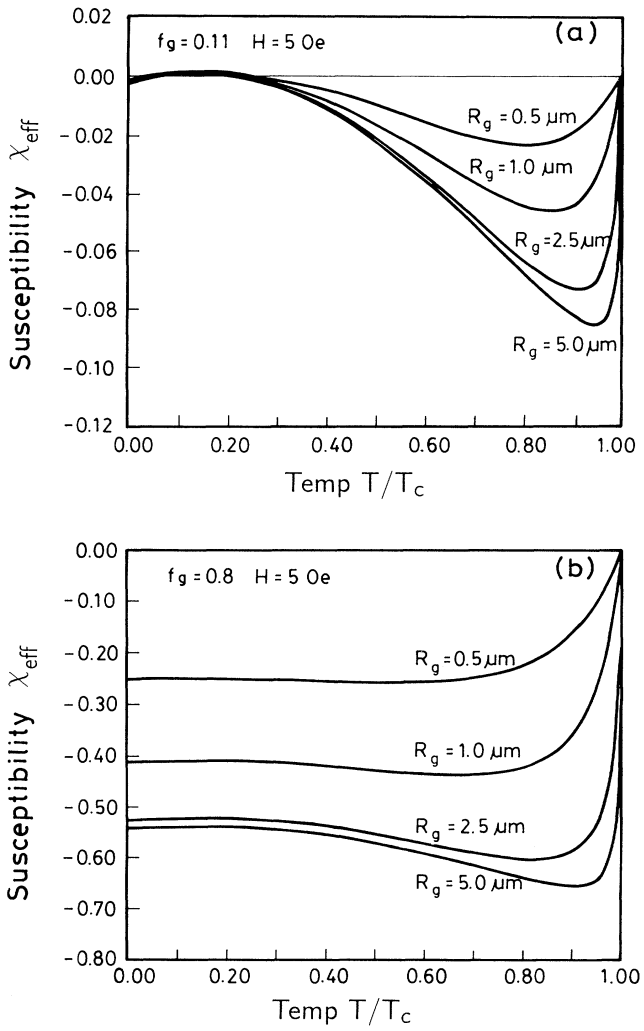

FIG. 7. The R_g dependence of field-cooled susceptibilities for $H=5$ Oe and (a) $f_g=0.11$ and (b) $f_g=0.8$, respectively.

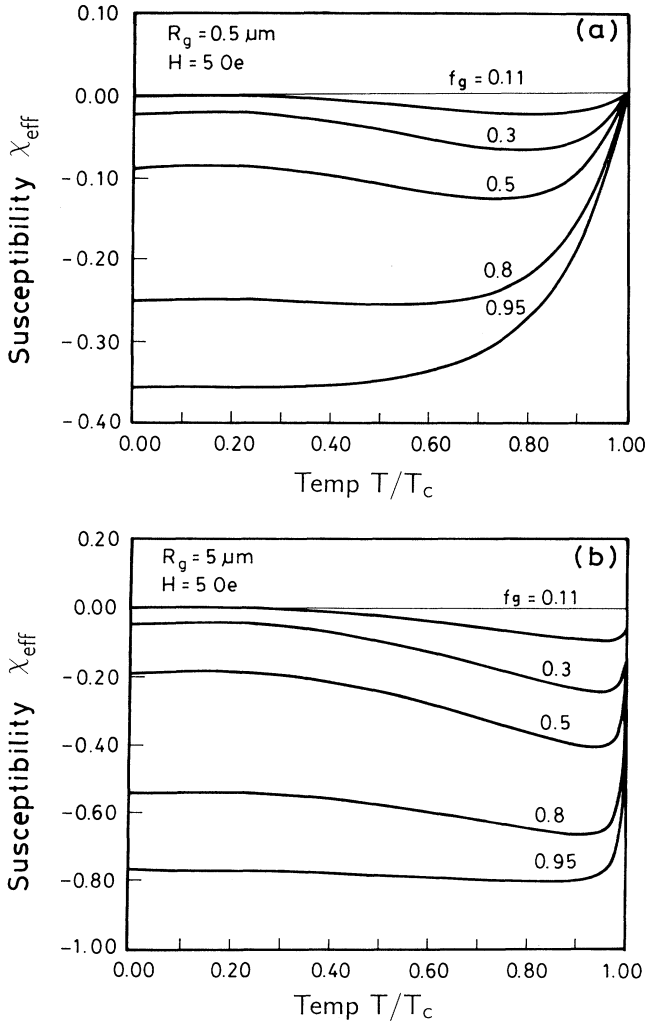

FIG. 8. The f_g dependence of field-cooled susceptibilities calculated by Eq. (14) with $H=5$ Oe and (a) $R_g=0.5$ μm and (b) $R_g=5$ μm, respectively.

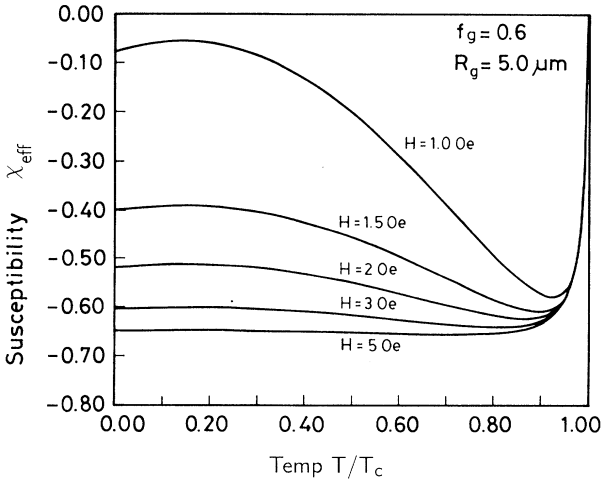

FIG. 9. The calculation result of χ_{eff} for $La_{1.85}Sr_{0.15}CuO_4$, shown in Fig. 1(a), with $R_g=5\ \mu m$, $f_g=0.6$.

full Meissner effect $\geq 40\%$ under a constant field of 10 Oe. This result is also consistent with the calculation of this model. Furthermore, a sample with $R_g=10\ \mu m$ and $0.5\leq f_g\leq 0.8$ would exhibit 53–65% of the perfect Meissner effect at $T/Tc=0.05$ under $H=20$ Oe on the basis of this model. This value is not in contradiction with those previously reported[31] in which the sample resembles R_g, f_g, and H and exhibits $\chi_{\text{eff}}\approx 55\%$.

This model is apparently not only suitable for the Y 1:2:4 bulks but may also be extended toward other systems, that is, if the elementary physical parameters including the $\lambda_{g,ab}(0)$, $\xi_{g,ab}(0)$, $H_{c1g}(0)$, and $H_{c2g}(0)$ are properly chosen for the calculated system. For example, the sample $La_{1.85}Sr0.15CuO_4$, shown in Fig. 1(a), has an average grain size of 10 μm and grain volume fraction of 0.6. The sample reported in Ref. 32 has $H_{c1}(0)\approx 5.2$ mT, $H_{c2}(0)\approx 40$ T, $\lambda(0)\approx 3330$ Å, and $\xi(0)\approx 30$ Å. The calculated result of the χ_{eff} for this sample indicates no positive moment to be observed for applied field larger than 5 Oe, as shown in Fig. 9, which is similar to the measured one.

IV. CONCLUSIONS

FC magnetization of the granular HTSC bulks was observed to possess an interesting dip phenomenon (Figs. 1 and 4) in the low magnetic-field regime, which is not already realized by the typical and well-known characteristics or previously published results on HTSC. A model was proposed in this work for theoretically interpreting this phenomenon and proving that it is an intrinsic feature of granular superconductors at the low field regime, caused by the paramagnetic induction of the intergranular region due to the intragranular supercurrents. The magnitude of the applied field required for an observation of the positive moment depends on the sample properties, such as the grain size and grain volume fraction.

ACKNOWLEDGMENTS

The authors would like to thank S. C. Wu, M. C. Hseih, J. S. Haung, and C. Y. Chen for their useful suggestions and W. K. Heish and M. W. Wang for their assistance on numerical computation. One of the authors (F.H.C) is also pleased to acknowledge assistance with the preparation of this manuscript with H. C. Lo. This study is supported by the National Science Council of R.O.C. under project No. NSC-81-0212-M009-518.

APPENDIX: CALCULATION OF PERMEABILITY OF INTERGRANULAR LAYERS INDUCED BY THE SUPERCURRENT

A fine and round conducting circle with a radius of r is indicated from Fig. 10 to be carried with current I. The circle is placed at xy plane and its center is located at $(x,y,z)=(0,0,0)$. The vector potential $\mathbf{A}$ can be found at (x,y,z), which is established by this current with the formula

$$\mathbf{A}=\frac{\mu_0 I}{4\pi}\oint_c \frac{d\mathbf{l}}{R_1}\ , \tag{A1}$$

with

$$d\mathbf{l}=dl\boldsymbol{\varphi}=rd\varphi\boldsymbol{\varphi}=rd\varphi(-\mathbf{x}\sin\varphi+\mathbf{y}\cos\varphi)\ , \tag{A2}$$

where $\mathbf{x}$ and $\mathbf{y}$ are the basis vectors in rectangular coordinate and $\mathbf{R}$, $\boldsymbol{\theta}$, and $\boldsymbol{\varphi}$ are the basis vectors in spherical coordinate. On the other hand,

$$\begin{aligned}R_1&=[(x-r\cos\varphi)^2+(y-r\sin\varphi)^2+z^2]^{1/2}\\&=[x^2+y^2+z^2+r^2-2r(x\cos\phi+y\sin\varphi)]^{1/2}\\&=R\left[1+\frac{r^2}{R^2}-\frac{2r}{R^2}(x\cos\varphi+y\sin\varphi)\right]^{1/2}\ ,\end{aligned} \tag{A3}$$

where $R=(x^2+y^2+z^2)^{1/2}$. If $R^2\gg r^2$,

$$R_1^{-1}\approx R^{-1}\left[1+\frac{rx}{R^2}\cos\varphi+\frac{ry}{R^2}\sin\varphi\right]\ . \tag{A4}$$

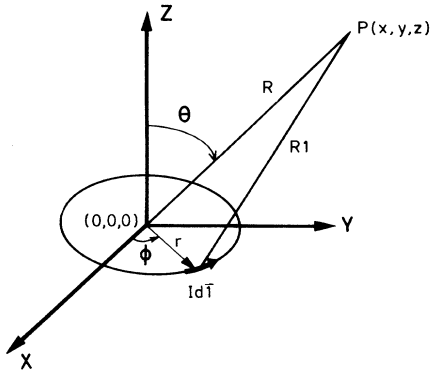

FIG. 10. The schematic configuration of a fine and round circle carrying with current I and establishing a magnetic field at (x,y,z).

Putting (A2) and (A4) into (A1) yields

$$\mathbf{A}=\frac{\mu_0 Ir^2}{4R^3}(-\mathbf{x}y+\mathbf{y}x)\ . \tag{A5}$$

According to the coordinate transformation, $x=R\sin\theta\cos\varphi$ and $y=R\sin\theta\sin\varphi$, (A5) can be rewritten as

$$\mathbf{A}=\boldsymbol{\varphi}\frac{\mu_0 Ir^2}{4R^2}\sin\theta=A_\varphi\boldsymbol{\varphi} \tag{A6}$$

where $A_\varphi=(\mu_0 Ir^2/4\mathbf{R}^2)\sin\theta$. Therefore,

$$\mathbf{B}=\nabla\times\mathbf{A}=\frac{\mathbf{R}}{R\sin\theta}\left[\frac{\partial}{\partial\theta}(A_\varphi\sin\theta)\right]-\frac{\boldsymbol{\theta}}{R}\left[\frac{\partial}{\partial R}(RA_\varphi)\right] \tag{A7}$$

$$=\frac{\mu_0 Ir^2}{4R^3}[(2\cos\theta)\mathbf{R}+(\sin\theta)\boldsymbol{\theta}]\ . \tag{A8}$$

For calculating the induction in xy plane, we only require that $\theta=90°$, i.e.,

$$B=\frac{\mu_0 Ir^2}{4R^3} \tag{A9}$$

and the permeability factor Q_m equals

$$Q_m=\frac{B}{H}=\frac{\mu_0 Ir^2}{4HR^3}\ . \tag{A10}$$

In this model, $R=R_g+d_n$ is established for estimating the average effect, where R_g is the cylinder grain's radius and d_n is the half thickness of intergranular layers.

*Author to whom correspondence should be addressed.

[1]L. Krusin-Elbaum, A. P. Malozemoff, Y. Yeshurun, D. C. Cronemeyer, and F. Holtzberg, Physica C **153-155**, 1460 (1988).
[2]V. V. Alexandrov, V. V. Borisovskii, T. A. Fedotova, L. M. Fisher, N. V. Il'in, O. K. Smirnova, I. F. Voloshin, M. A. Baranov, and V. S. Gorbachev, Physica C **173**, 458 (1991).
[3]A. P. Malozemoff, L. Krusin-Elbaum, D. C. Cronemeyer, Y. Yeshurun, and F. Holtzberg, Phys. Rev. B **38**, 6490 (1988).
[4]K. A. Müller, M. Takashige, and J. G. Bednorz, Phys. Rev. Lett. **58**, 1143 (1987).
[5]J. R. Clem, Physica C **153-155**, 50 (1988).
[6]K.-H. Muller, Physica C **159**, 717 (1989).
[7]W. H. Lee, Y. T. Haung, S. W. Lu, K. Chen, and P. T. Wu, Solid State Commun. **74**, 97 (1990).
[8]F. J. Blunt, A. R. Perry, A. M. Campbell, and R. S. Liu, Physica C **175**, 539 (1991).
[9]M. F. Tai, H. J. Wang, C. C. Lin, and H. L. Wang, in MRS Symposia Proceedings No. 275 (Materials Research Society, Pittsburgh, 1992).
[10]H. J. Wang and M. F. Tai (unpublished work).
[11]M. H. Tai (private communication).
[12]S. Jin, H. M. O'Bryan, P. K. Gallagher, T. H. Teifel, R. J. Cava, R. A. Fastnacht, and G. W. Kammlott, Physica C **165**, 415 (1990).
[13]D. M. Pooke, R. G. Buckley, M. R. Presland, and J. L. Tallon, Phys. Rev. B **41**, 6616 (1990).
[14]S. C. Wu, F. H. Chen, H. S. Koo, M. F. Tai, and T. Y. Tseng (unpublished).
[15]J. Karpinski, E. Kaldis, E. Jilek, S. Rusiechi, and B. Bucher, Nature (London) **336**, 660 (1988).
[16]D. E. Morris, J. H. Nickel, J. Y. T. Wei, N. G. Asmer, J. S. Scott, V. M. Scheven, C. T. Hultgren, A. G. Markelz, J. E. Post, D. J. Heaney, D. R. Veblen, and R. M. Hazen, Phys. Rev. B **39**, 7347 (1989).
[17]D.-X. Chen, J. Nogues, and K. V. Rao, J. Appl. Phys. **64**, 2533 (1988).
[18]V. Skumryev, M. R. Koblischka, and H. Kronmüler, Physica C **184**, 332 (1991).
[19]H. Küpfer, I. Apfelstedt, R. Flukiger, C. Keller, R. Meier-Hirmer, B. Runtsch, A. Turowski, U. Wiech, and T. Wolf, Cryogenics **28**, 650 (1988).
[20]D.-X. Chen, J. Nogues, and K. V. Rao, Cryogenics **29**, 800 (1989).
[21]Y. B. Kim, C. F. Hempstead, and A. R. Strnad, Phys. Rev. Lett. **9**, 306 (1962).
[22]H. Dersch and G. Blatter, Phys. Rev. B **38**, 11 391 (1988).
[23]P. Chaddah, G. Ravi Kumar, A. K. Grover, C. Rhadakrishnamurty, and G. V. Subba Rao, Cryogenics **29**, 907 (1989).
[24]A. A. Zhukov, V. V. Moshchalkov, D. A. Komarkov, V. P. Shabatin, A. A. Bush, S. N. Gordeev, and D. V. Shelomov, Physica C **162-164**, 1623 (1989).
[25]J. R. Clem and V. G Kogan, Jpn. J. Appl. Phys. **26**, 1161 (1987).
[26]M. W. Coffey and J. R. Clem, Phys. Rev. B **45**, 9872 (1992).
[27]M. Tinkham, *Introduction to Superconductivity* (McGraw-Hill, New York, 1975), p. 113.
[28]J. C. Martinez, J. J. Prejean, J. Karpinski, E. Kaldis, and P. Bordet, Solid State Commun. **75**, 315 (1990).
[29]W. C. Lee and D. M. Ginsberg, Phys. Rev. B **45**, 7402 (1992).
[30]T. Wada, N. Suzuki, A. Ichinose, Y. Yaegashi, H. Yamauchi, and S. Tanaka, Jpn. J. Appl. Phys. **29**, L915 (1990).
[31]G. Triscone, T. Graf, A. Junod, D. Scanchez, O. Brunner, D. Cattani, and J. Muller, Physica C **168**, 40 (1990).
[32]D. K. Finnemore, R. N. Shelton, J. R. Clem, R. W. McCallum, H. C. Ku, R. E. McCarley, S. C. Chen, P. Klavins, and V. Kogan, Phys. Rev. B **35**, 5319 (1987).

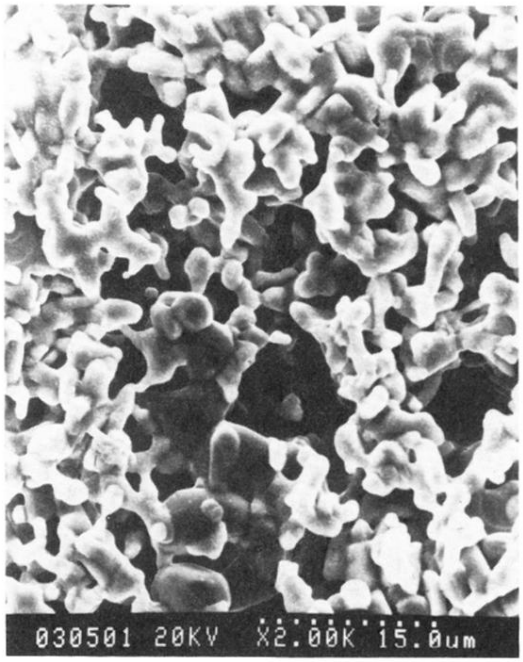

FIG. 2. The SEM micrograph for 1:2:4 compounds prepared by the sol-gel method and sintering at ambient atmosphere.